

SEVEN NEW LOW-MASS ECLIPSING BINARIES

JEFFREY L. COUGHLIN

Department of Astronomy New Mexico State University Las Cruces, NM 88003 USA

AND

J. SCOTT SHAW

Department of Physics and Astronomy University of Georgia Athens, GA 30602 USA

ABSTRACT

We present the discovery of seven new low-mass eclipsing binaries, their photometric light curves, and preliminary models. This nearly doubles the available data on these systems, with only nine previously known. Once radial-velocity curves are completed, physical parameters will be determined with an error of less than 2-3%, thus allowing for a rigorous examination of stellar models in the lower-main sequence. Our initial analysis seems to support the current findings that low-mass stars have greater radii than models predict, most likely due to the presence of strong magnetic fields.

Subject headings: binaries: eclipsing – stars: low mass, brown dwarfs

1. INTRODUCTION

Binary stars form the fundamental basis of stellar astronomy in the sense that they are the primary means to observationally determine the physical parameters of stars. These quantities can then be tested against the predictions of various stellar models to learn something interesting about the underlying physics. Recently, much progress has been made in determining the physical parameters of stars on the lower main sequence, for which numerous stellar models already exist (Siess et al. 1997, Baraffe et al. 1998, Yi et al. 2001). Also referred to as low-mass stars, they are defined as having less than one solar mass and effective temperatures of less than 6000K. Being intrinsically faint they are difficult to detect. Before 2003, only three low-mass systems were known: YY Gem (Torres & Ribas 2002; Leung & Schneider 1978), CM Dra (Metcalf et al. 1996), and CU Cnc (Delfosse et al. 1999; Ribas 2003). Since then, the number of known systems has tripled to include OGLE BW5V038 (Maceroni & Montalbán 2004), GU Boo (López-Morales & Ribas 2005), TrES-Her0-07621 (Creedy et al. 2005), EMTSS-6 [RXJ0239.1-1028] (Torres et al. 2006), 2MASS J05162881+2607387 (Bayless & Orosz, priv. comm.), and NSVS01031772 (Lopez-Morales et al., in prep.).

Still, a total of nine systems is not an adequate amount of data to definitively test the various stellar models. It is to this end that we present the discovery, photometric light curves, and preliminary models of seven new low-mass systems found from the Northern Sky Variability Survey (NSVS) (Wozniak et al. 2004). They are NSVS01286630 [$14^h 47^m 09^s$, $+78^\circ 42' 33''$ (J2000)], NSVS02502726 [$08^h 44^m 11^s$, $+54^\circ 23' 48''$ (J2000)], NSVS06507557 [$01^h 58^m 24^s$, $+25^\circ 21' 19''$ (J2000)], NSVS07394765 [$08^h 25^m 51^s$, $+24^\circ 27' 05''$ (J2000)], NSVS07453183 [$09^h 16^m 12^s$, $+36^\circ 15' 32''$ (J2000)], NSVS10653195 [$16^h 07^m 28^s$, $+12^\circ 13' 59''$ (J2000)], and NSVS11868841 [$23^h 17^m 58^s$, $+19^\circ 17' 03''$ (J2000)]. Once radial-velocity curves are completed for each star, absolute physical parameters will be able to be extracted, nearly doubling the size of the existing dataset.

TABLE 1
CALCULATED PERIODS AND EPOCHS

Star	Period (days)	T0 (HJD)
NSVS01286630	0.3830 ± 0.0002	2453879.8030 ± 0.0003
NSVS02502726	0.559772 ± 0.000007	2453692.0280 ± 0.0003
NSVS06507557	0.5150895 ± 0.0000008	2453312.3722 ± 0.0005
NSVS07394765	2.26560 ± 0.00009	2453730.7303 ± 0.0002
NSVS07453183	0.366971 ± 0.000002	2453456.6763 ± 0.0002
NSVS10653195	0.560721 ± 0.000003	2453274.1720 ± 0.0030
NSVS11868841	0.60179 ± 0.00001	2453663.0257 ± 0.0004

2. PROCEDURE

2.1. Identification

Initial identification of candidates was performed by searching the NSVS data with two period-searching methods: the string/rope method based on the Lafler-Kinman statistic (Clarke 2002) and the analysis of variance method (Schwarzenberg-Czerney 1989). Colors were obtained from the 2 Micron All Sky Survey (2MASS) (Skrutskie et al. 2006), and from the Naval Observatory Merged Astrometric Dataset (NOMAD) (Zacharias et al. 2004). Once a candidate was confirmed to be a detached, low-mass system, high-precision light curves in the Johnson V, R, and I filters were obtained with the Southeastern Association for Research in Astronomy (SARA) 0.9 meter telescope at Kitt Peak National Observatory. After reduction, a total of 8,831 magnitude measurements were obtained, thus averaging 420 points per color curve.

2.2. Period and Epoch Determination

Times of minima were computed via the method of Kwee-van Woerden (Kwee & van Worden 1956). Periods and epochs, shown in Table 1, were calculated for each system using a least squares fit.

2.3. Temperature Determination

Magnitude measurements in B, V, R, and I were obtained from the USNO NOMAD catalogue, and J, H, and K_S , from the 2MASS catalogue, for each star. Color indices were computed for V-K, H-K, B-V, V-R, V-I, and J-K, and corresponding temperatures extrapolated from best-fits to the standard

tables of Houdashelt et al. (2000) and Tokunaga (2000). The effective temperature of the hotter component was set as the average of these measurements, shown in Table 2. We estimate the error in these temperatures to be $\pm 300\text{K}$, and will have to await the completion of spectra for more accurate determinations.

2.4. Mass Ratio and Separation Determination

Since radial velocity curves are not yet available, the scale of the binary system, and thus the mass ratio and separation, are not directly determinable. After running a few solutions to determine the temperature ratio of each system we decided to fix their masses, which allowed for a computation of both the mass ratio and orbital separation to be used in the final solutions. We used reference temperatures and corresponding masses from the model of Baraffe et al. (1998), with $[M/H] = 0$ and an age of 0.3 Gyrs. However, after the final solutions had been run, it was evident that each component's mass had been underestimated. To correct for this, we afterward fixed the masses based only on the 2MASS colors, which gave higher average temperatures, and thus larger masses. New orbital separations were computed, and multiplied by the effective radii found previously in the final solutions to compute absolute radii. Once spectra are obtained, this will not be an issue as mass will be determined from the radial velocity curves.

2.5. Modeling

Modeling of the seven new low-mass systems was performed via the Eclipsing Light Curve (ELC) program, written by J. A. Orosz (2000). The optimization routine used was geneticELC, which uses a genetic algorithm to find a best fit, based on the code of P. Charbonneau (1995). Light curves for an initial population of solutions, generated with random parameters, are computed and compared to the observational light curve. Their corresponding chi-squared value is used as a measure of fitness for natural selection, with parameters from good fits being passed on to a second generation of solutions, and parameters from bad fits being eliminated. After being subject to random mutations, to maintain parameter diversity, this second generation is compared to the observational data, and bred into a third generation of solutions. The process continues for N generations, until a satisfactorily low chi-squared is found. Thus, a large population ensures a complete exploration of the parameter space, and a large number of generations ensures that the global minimum chi-squared, or absolute best fit, is found.

For our final solutions, a total of 7200 points were distributed equally over the surface of each star, thus ensuring adequate spatial resolution during flux integration. Each light curve was computed with a total of 720 points, permitting sufficient phase resolution for the chi-squared computation. Initial solutions were run with the genetic ELC code with 100 population members for 100 generations, and final solutions were run with 50 population members for 100 generations with more highly constrained parameters. Thus, over 15,000 solutions were computed for each system, the best one of which is used.

A difficulty encountered in modeling these systems was the high level of spot activity that occurs in low-mass stars. Spot variation over the timeline of the observations account for a majority of the scatter in the data. For our final solutions, we assumed two cool spots, both on the hotter component, star 2. Although it is certainly an over-simplification when

dealing with these stars, we feel it is the only way to keep the solutions meaningful. For NSVS06507557, the spot shift was so extreme between groups of observing runs that two separate solutions for its spots were found; one for the data taken between JD 2453312 - 2453372, hereafter referred to as "300," and one for the data taken between JD 2453663 - 2453734, hereafter referred to as "600."

Please note that for NSVS11868841, only the V and R light curves were used for modeling, since at the very low light levels of this system a faint fringe pattern on the CCD introduced a noticeable noise in that filter.

3. RESULTS

3.1. ELC System Parameters

ELC defines star 1 as the star that is closest to the observer at primary, or phase zero, and thus star 2 is eclipsed at that time. For these systems then, star 2 is always the hotter component. T_1 and T_2 are the effective temperatures of star 1 and star 2 respectively. The mass ratio, Q , is the mass of star 2 divided by the mass of star 1. The orbital separation (Sep.), is defined as the distance between the two components' centers of mass. The inclination of the system is designated by i , with 90 degrees being an exactly edge-on orbit. The effective radii, $R_{\text{eff}1}$ and $R_{\text{eff}2}$, are the radius of star 1 and star 2 respectively divided by the orbital separation. For the spot parameters, TF_1 and TF_2 are the temperature factors, or ratio of the spot temperature to the underlying temperature, of spots 1 and 2. Rad_1 and Rad_2 are the radii of the spots, where 90 degrees covers exactly half the star. Lat_1 , Lat_2 , Lon_1 , and Lon_2 are the respective latitudes and longitudes of spots 1 and 2. The north pole is at a latitude of 0 degrees, the equator at 90 degrees, and the south pole at 180 degrees. The longitude is zero degrees at the inner Lagrangian point, 90 degrees on the leading side, 180 degrees at the back end, and 270 degrees on the trailing side. The physical values for each system used in or derived from the final solutions of the ELC program are shown in Tables 3 and 4.

3.2. Light Curve Fits and Visual Models

Observed light curves and models from ELC are shown in Figures 1 - 8. The I-filter light curve is on top, followed by the R-filter in the middle, and the V-filter on the bottom, with the best-fit solution shown as a solid line through the data. The models are a grayscale representation of temperature, with darker regions representing cooler temperatures, and lighter regions representing hotter temperatures.

3.3. Mass-Radius Relation

The computed physical mass and radius for each star is shown in Table 5, although it should be stressed that without optical spectroscopy these are based on assigned masses extrapolated from their temperatures. M_1 , M_2 , R_1 , and R_2 are the mass and radius of star 1 and star 2 respectively in each system. A graph of this data is shown alongside previous data and the leading stellar model in Figure 9.

4. DISCUSSION

The most striking feature of these systems is their high level of spot activity. In several of the light curves, which were compiled in a time span ranging from a few days to two years, one can see where the light curves from different nights differ by about 0.01 mag. This is due to rapid spot movement or change between two observing runs. The most notable

TABLE 2
CALCULATED EFFECTIVE TEMPERATURES

Star	Avg. Teff (K)		V-K	H-K	B-V	V-R	V-I	J-K
NSVS01286630	4290	Index (Mag)	2.608	0.148	1.200	0.730	1.550	0.653
		Temp (K)	4450	4060	4170	4230	4040	4770
NSVS02502726	4370	Index (Mag)	2.564	0.154	1.260	0.500	1.450	0.738
		Temp (K)	4530	4000	4030	4980	4160	4530
NSVS06507557	3860	Index (Mag)	3.278	0.175	1.360	1.010	2.130	0.826
		Temp (K)	4050	3810	3800	3680	3530	4310
NSVS07394765	3570	Index (Mag)	8.250	0.160	0.380	6.550	6.750	0.834
		Temp (K)	2660	3940	6730	1640	2160	4290
NSVS07453183	4120	Index (Mag)	2.672	0.132	1.570	0.930	1.400	0.692
		Temp (K)	4450	4230	3360	3800	4220	4660
NSVS10653195	3970	Index (Mag)	3.393	0.160	1.210	1.070	1.840	0.779
		Temp (K)	3990	3940	4150	3580	3750	4420
NSVS11868841	4910	Index (Mag)	1.875	0.074	1.120	0.610	1.010	0.523
		Temp (K)	5230	5250	4370	4570	4850	5210

TABLE 3
ORBITAL ELEMENTS FOR EACH OF THE SEVEN SYSTEMS

Star	Period (Days)	T ₁ (K)	T ₂ (K)	M ₁ +M ₂ (M _⊙)	Q	Sep. (R _⊙)	i (°)	Reff ₁	Reff ₂
NSVS01286630	0.3830	4140	4290	1.405	1.05	2.48	89.0	0.33	0.35
NSVS02502726	0.559772	3950	4370	1.259	1.20	3.09	88.2	0.24	0.27
NSVS06507557	0.5150895	3210	3860	1.259	2.52	2.60	84.1	0.16	0.24
NSVS07394765	2.26560	3170	3860	0.893	1.16	2.60	84.1	0.18	0.2
NSVS07453183	0.366971	3340	3570	1.216	1.07	7.75	89.1	0.08	0.09
NSVS10653195	0.560721	3920	4120	1.406	1.10	2.42	85.4	0.30	0.33
NSVS11868841	0.60179	3750	3970	1.278	1.08	3.10	87.5	0.22	0.25

TABLE 4
SPOT PARAMETERS FOR EACH OF THE SEVEN SYSTEMS

Star	TF ₁	Lat ₁	Lon ₁	Rad ₁	TF ₂	Lat ₂	Lon ₂	Rad ₂
NSVS01286630	0.86	154	349	46	0.88	21	124	37
NSVS02502726	0.95	30	22	30	0.95	5	284	52
NSVS06507557 (300)	0.94	132	2	6	0.94	178	72	90
NSVS06507557 (600)	0.95	41	107	44	0.94	164	21	85
NSVS07394765	0.89	28	273	33	0.94	21	163	56
NSVS07453183	0.83	31	29	21	0.98	55	332	79
NSVS10653195	0.93	161	44	87	0.98	68	157	70
NSVS11868841	0.65	172	22	50	0.79	1	137	60

TABLE 5
CALCULATED PHYSICAL MASS AND RADIUS FOR THE SEVEN SYSTEMS

Star	M ₁ (M _⊙)	M ₂ (M _⊙)	R ₁ (R _⊙)	R ₂ (R _⊙)
NSVS01286630	0.68	0.72	0.81	0.87
NSVS02502726	0.57	0.69	0.75	0.83
NSVS06507557	0.25	0.64	0.40	0.61
NSVS07394765	0.56	0.65	0.58	0.69
NSVS07453183	0.68	0.73	0.72	0.79
NSVS10653195	0.61	0.67	0.67	0.79
NSVS11868841	0.87	0.94	0.93	1.03

system, NSVS06507557, shows major change over both the

course of a year and a month. The yearly cycle is evidenced by the separation of the 300 and 600 light curves, which vastly differ. The month time scale is demonstrated in the 300 light curve by the noticeably different secondary eclipse in the R filter, and the shoulder after primary in the I filter. These observations were taken a month before the rest of the 300 curve. Comparing the solutions for the 300 and 600 curves, we find that while both the spots stayed the same temperature, one may have shifted only slightly from its original position, while the other moved between hemispheres and grew tremendously in size. However, the physical validity of this model is questionable, and it should be stressed that spot modeling was only introduced to add symmetry to the light curve and obtain a more accurate determination of mass and temperature, not to evaluate low-mass star spot cycles. However, the

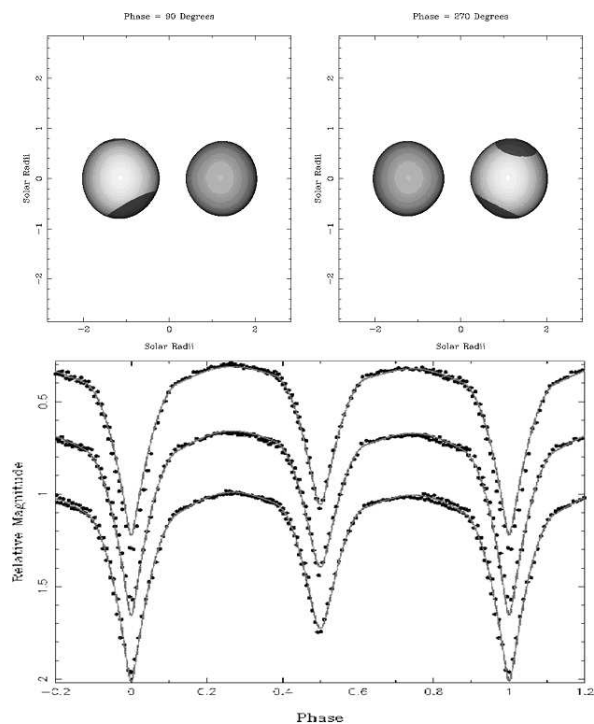


FIG. 1.— NSVS01286630. Top: ELC Model. Star 1 is on the right at phase 90. Bottom: Light Curves (I-top, R-middle, V-bottom) with Model Fit (Solid Line).

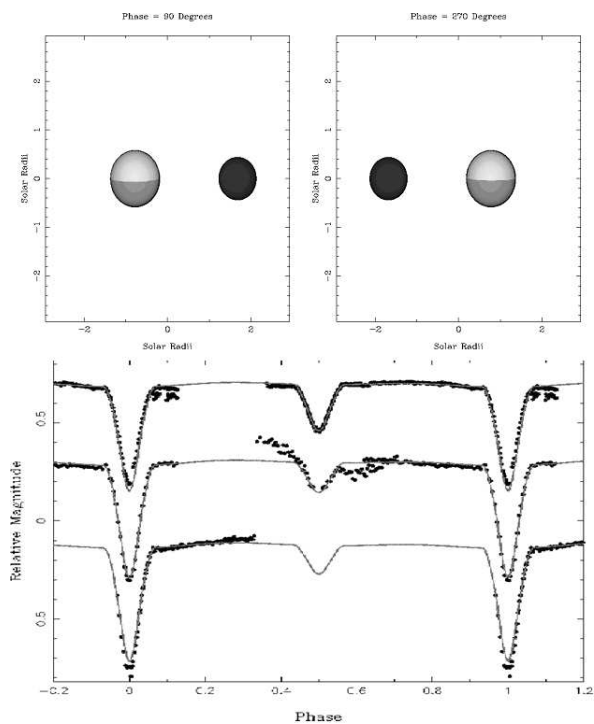


FIG. 3.— NSVS06507557 (300). Top: Model. Star 1 is on the right at phase 90. Bottom: Light Curves (I-top, R-middle, V-bottom) with Model Fit (Solid Line).

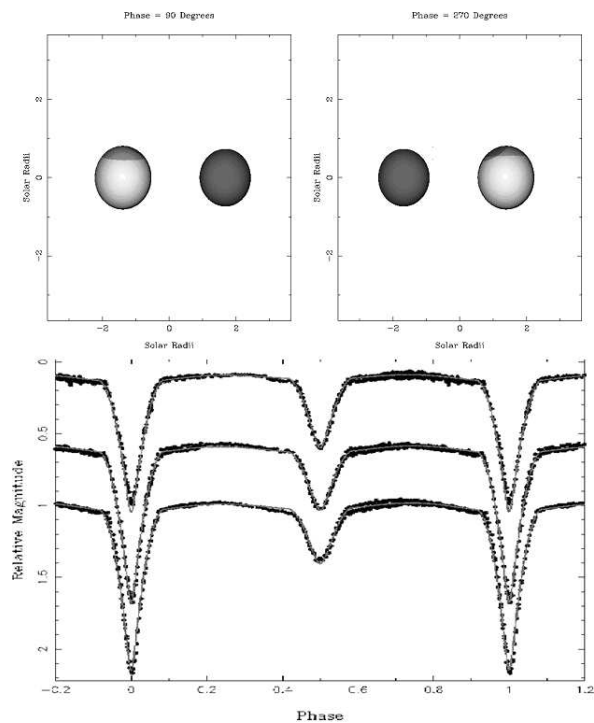


FIG. 2.— NSVS02502726. Top: ELC Model. Star 1 is on the right at phase 90. Bottom: Light Curves (I-top, R-middle, V-bottom) with Model Fit (Solid Line).

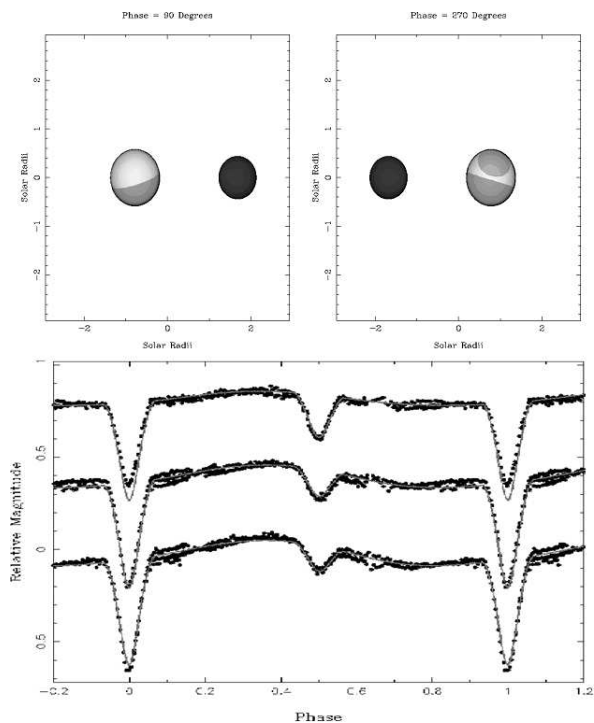


FIG. 4.— NSVS06507557 (600). Top: Model. Star 1 is on the right at phase 90. Bottom: Light Curves (I-top, R-middle, V-bottom) with Model Fit (Solid Line).

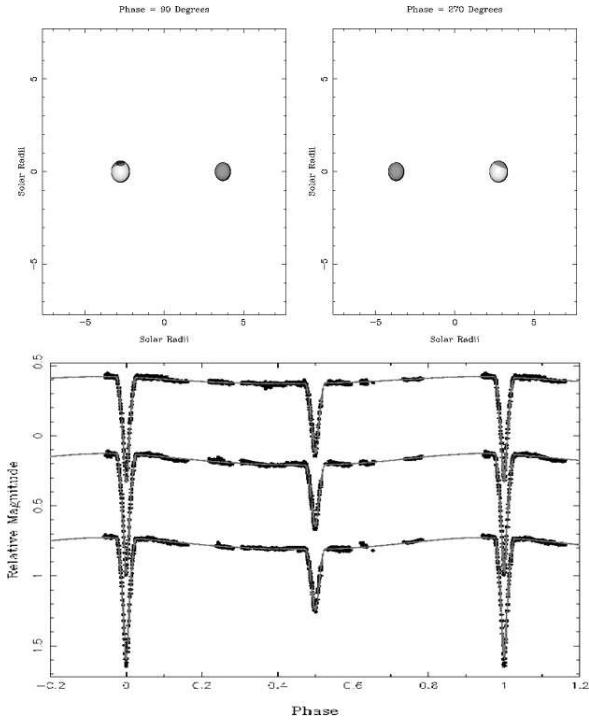


FIG. 5.— NSVS07394765. Top: ELC Model. Star 1 is on the right at phase 90. Bottom: Light Curves (I-top, R-middle, V-bottom) with Model Fit (Solid Line).

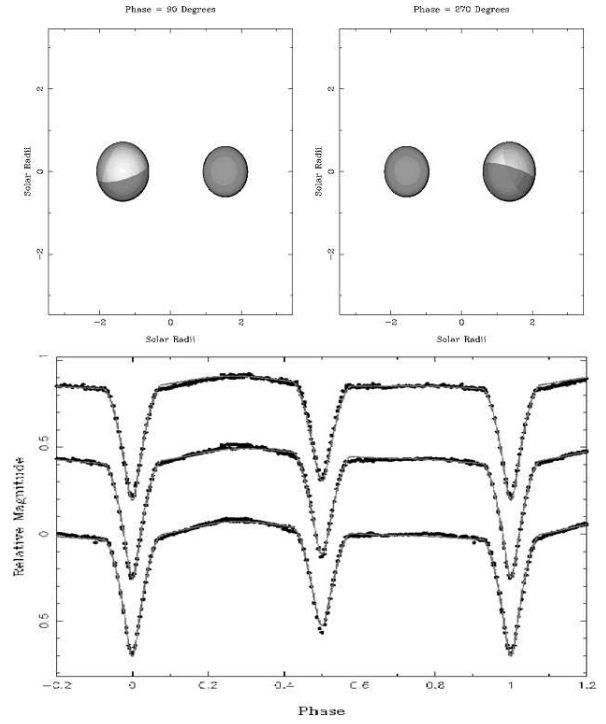


FIG. 7.— NSVS10653195. Top: ELC Model. Star 1 is on the right at phase 90. Bottom: Light Curves (I-top, R-middle, V-bottom) with Model Fit (Solid Line).

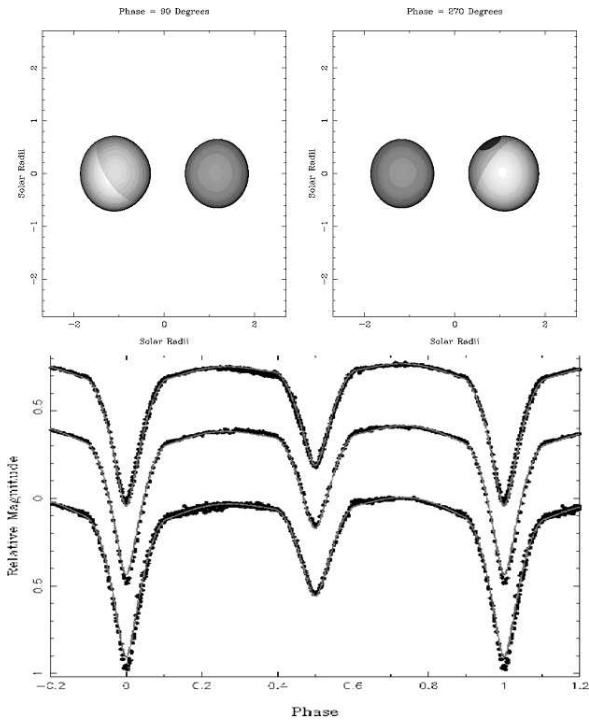


FIG. 6.— NSVS07453183. Top: ELC Model. Star 1 is on the right at phase 90. Bottom: Light Curves (I-top, R-middle, V-bottom) with Model Fit (Solid Line).

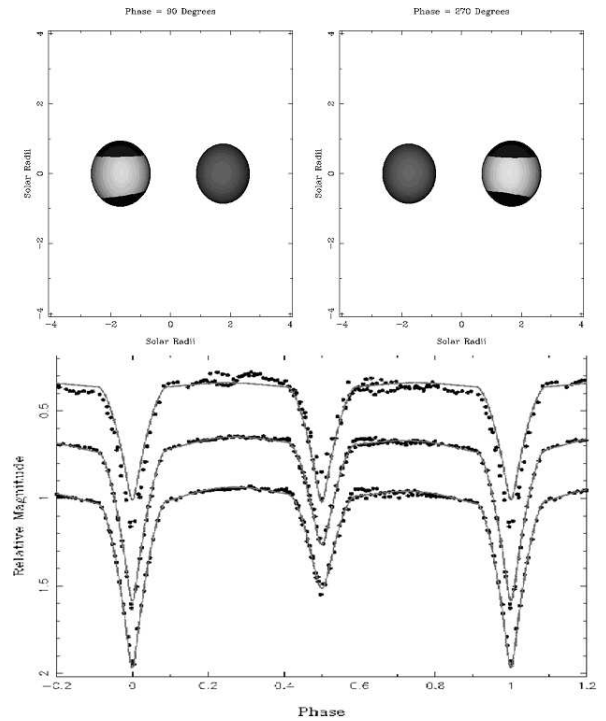


FIG. 8.— NSVS11868841. Top: ELC Model. Star 1 is on the right at phase 90. Bottom: Light Curves (I-top, R-middle, V-bottom) with Model Fit (Solid Line).

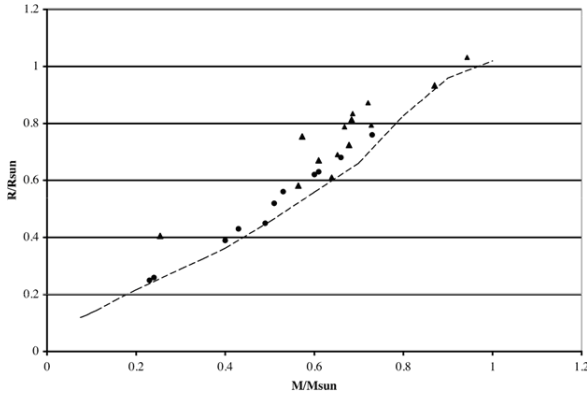


FIG. 9.— Mass-Radius relation for the seven new systems (triangles), plus the nine previously known systems (circles) from López-Morales and Shaw (2006). The model of Baraffe (1998) with $[M/H] = 0$ and an age of 0.3 Gyrs is shown by the dashed line.

presence itself of strong and rapidly changing spots illustrates the high strength of the magnetic fields at work in these stars, and lends credence to the suggestion that this is the cause of the "oversized" radii.

We have plotted the seven new systems with previous data in a M-R diagram in Figure 9. Even without optical spectroscopy the new systems seem to follow the trend of previous data, and supports the idea that these stars have a larger radius than theory predicts.

5. CONCLUSIONS

We have presented the discovery, light curves, and basic orbital parameters for seven new low-mass eclipsing binary

systems. The preliminary models seem to support the most recent findings that low-mass stars have a greater radius than current models predict. The high-level of spot activity found supports the idea that strong magnetic fields are responsible for the large radii. Optical spectroscopy is needed to determine the sizes and masses of these objects to within a 2-3% error, which is needed to definitively distinguish between the predictions of current stellar models for the lower main-sequence.

The authors would like to thank the NSF and DoD for their generous support. This work was funded by a partnership between the National Science Foundation (NSF AST-0552798) Research Experiences for Undergraduates (REU) and the Department of Defense (DoD) ASSURE (Awards to Stimulate and Support Undergraduate Research Experiences) programs.

This publication makes use of data products from the Two Micron All Sky Survey, which is a joint project of the University of Massachusetts and the Infrared Processing and Analysis Center/California Institute of Technology, funded by the National Aeronautics and Space Administration and the National Science Foundation.

This research has made use of the USNOFS Image and Catalogue Archive operated by the United States Naval Observatory, Flagstaff Station (www.nofs.navy.mil/data/fchpix/).

REFERENCES

- Baraffe, I.; Chabrier, G.; Allard, F., and Hauschildt, P. H. 1998, *A&A*, 337, 403
 Bayless, A. and Orosz J. 2006, private communication
 Charbonneau, P. 1995, *ApJS*, 101, 309
 Clarke, D. 2002 *A&A*, 386, 763
 Creevey, O. L., et al. 2005, *ApJ*, 625, L127
 Delfosse, X.; Forveille, T.; Mayor, M.; Burnet, M., and Perrier, C. 1999, *A&A* 341, L63
 Houdashelt, B., and Sweigart, A. J., March, 2000
 Kwee, K. K., and van Woerden, H. 1956, *B.A.N.*, 12, 464
 Leung, K. C., and Schneider, D. P. 1978, *AJ*, 83, 618
 López-Morales, M., and Ribas, I. 2005, *ApJ*, 631, 1120
 López-Morales, M., and Shaw, J. S. 2006, *ASP Conference Series*
 Maceroni, C., and Montalbán 2004 *A&A* 426, 577
 Metcalfe, T. S.; Mathieu, R. D.; Latham, D. W., and Torres, G. 1996, *ApJ*, 456, 356
 Orosz, J. A., and Hauschildt, P.H. 2000, *A&A*, 364, 265
 Ribas, I. 2003, *A&A*, 398, 239
 Siess, L.; Forestini, M., and Dougados, C. 1997, *A&A*, 324, 556
 Schwarzenberg-Czerney, A. 1989, *MNRAS*, 241, 153
 The Two Micron All Sky Survey (2MASS)
 Skrutskie, M. F., et al. 2006, *AJ*, 131, 1163.
 Tokunaga, A.T.; Allen's Astrophysical Quantities, 4th edition; Springer-Verlag (New York); 2000; pp. 143.
 Torres G. 2006, private communication
 Torres, G., and Ribas, I. 2002, *ApJ*, 567, 1140
 Wozniak, P. R., et al. 2004, *AJ*, 127, 2436
 Yi, S., et al. 2001, *ApJS*, 136, 417
 Zacharias, N.; Monet, D. G.; Levine, S. E.; Urban, S. E.; Gaume, R., and Wycoff, G.L., 2004, *AAS* 205